

DOI: 10.24425/amm.2019.127561

R. RUMMAN^{*#}, D.A. LEWIS^{*}, J.Y. HASCOET^{**}, J.S. QUINTON^{*}**LASER METAL DEPOSITION AND WIRE ARC ADDITIVE MANUFACTURING OF MATERIALS: AN OVERVIEW**

Additive manufacturing (AM) is a process that joins similar or dissimilar materials into application-oriented objects in a wide range of sizes and shapes. This article presents an overview of two additive manufacturing techniques; namely Laser metal deposition (LMD) and Wire arc additive manufacturing (WAAM). In LMD, metallic powders are contained in one or more chambers, which are then channelled through deposition nozzles. A laser heats the particles to produce metallic beads, which are deposited in layers with the aid of an in-built motion system. In WAAM, a high voltage electric arc functions as the heat source, which helps with ensuring deposition of materials, while materials in wire form are used for the feedstock. This article highlights some of the strengths and challenges that are offered by both processes. As part of the authors' original research work, Ti-6Al-4V, Stainless steel 316L and Al-12Si were prepared using LMD, while the WAAM technique was used to prepare two Al alloys; Al-5356 and CuAl₈Ni₂. Microstructural analysis will focus on similarity and differences in grains that are formed in layers. This article will also offer an overall comparison on how these samples compare with other materials that have been prepared using LMD and WAAM.

Keywords: Additive manufacturing, laser metal deposition, wire arc, microstructure.

1. Introduction

3D or three dimensional printing is one of the novel technologies that can completely change the way conventional manufacturing is outlined within aerospace, aviation, medical, maritime and other prominent industries [1]. The use of this technology offers a significantly higher degree of customisation and personalisation to a wide range of products. It also offers lower design and manufacturing costs for application-oriented composites and alloys. In a broader sense, 3D printing allows new ways to work with several types of materials; from metals to ceramics and polymers to living cells. Depending on factors involved in the process, such as type of material, speed of production, printing resolution, surface finish, melting and joining mechanism, thermal memory, supply of raw materials and feedstock, a number of different approaches to additive 3D printing processes have evolved over the past two decades. One thing these processes have in common is the construction of layered objects, which allow room for manufacturing complex structures that are difficult to achieve through conventional subtractive manufacturing. Additive manufacturing methods that focus on metal-based composites are divided into two categories; namely powder bed fusion (PBF) where metallic powders are melted in layers, and directed energy deposition (DED), where a 'welding' heat source is used to melt metals in wire or powder form to create deposited metallic layers.

Laser metal deposition (LMD), also known as laser solid forming (LSF) or direct metal deposition (DMD) is one of the most recent 3D printing processes and is capable of building high density metallic alloys from powders without the need of a mould or tool [2-5]. A significant advantage of LMD is the greater flexibility and control it offers in terms of controlling the heat input. The process uses a laser to provide the heat energy source to melt powder metals, which are then deposited onto the desired surface. With the help of 3-D CAD modelling, this layer by layer structure finally creates the desired object, ensuring strong metallurgical bonding between the surfaces [6]. As the process involved typically creates the object through layering of materials, the large surface areas as well as substrate heat dissipation allow for a fast cooling rate, which is another reason why LMD has gained popularity. In contrast with subtractive manufacturing, LMD significantly reduces material wastage, which also brings manufacturing costs down, even for complex structures. In addition, the optimisation of substrate-particle contact time, contact shape and area, and temperature in this process can ensure an extremely high degree of adhesion between layers in 3D printed materials. One of the biggest advantages of the process is that it can use elemental or composite particles for the manufacture of products, which makes it possible to work with any composition, and can cater any industry in all true sense. The greater flexibility in terms of heat input also extends the capability in manufacturing high temperature materials like

* FLINDERS UNIVERSITY, INSTITUTE FOR NANOSCALE SCIENCE AND TECHNOLOGY, ADELAIDE, SOUTH AUSTRALIA

** ECOLE CENTRALE DE NANTES, GEM, UMR CNRS 6183 FRANCE

Corresponding author: Raihan.rumman@flinders.edu.au

refractory alloys. In addition, the process is equipped to, and can be extensively used as a repair technology, unlike most conventional and emerging methods, potentially benefiting highly sensitive industries like aviation and aerospace. In contrast, one of the limiting factors of this method is the contamination of particles, which is why industries tend to use dedicated machines for certain range and type of materials. Also, the use of control parameters to ensure proper melting of all particles along fusion bands can be difficult to achieve, especially in compositions that are hard to locally sinter through rapid diffusion mechanism.

Another developing additive manufacturing method that has recently attracted considerable interest is wire and arc additive manufacturing (WAAM), [7-10]. In this process, an electric arc acts as the heat source while a wire is used as the feedstock, allowing large component production at a high deposition rate [11]. Normally low cost solutions like gas metal arc welding or tungsten based gas welding are used as the heat source, which works towards achieving the high deposition rate. Although a number of feedstock materials have been tried and tested in WAAM, Titanium alloys have been quite successful in achieving large-scale production as well as the mechanical property requirements. In WAAM, rapid heating of materials causing faster diffusion, repeated heating cycles, and anisotropic heat extraction, can complicate the mechanical behaviour and microstructural features of materials. To address these challenges, in addition to varying processing parameters and inoculation, a post processing heat treatment has been extensively used for WAAM-manufactured components. One of the other critical challenges is to constantly find ways to supply materials and new compositions in wire form. While it can be achieved for softer alloys or alloys containing a softer binder, hard to machine materials including

refractory alloys have not seen success with this technology. In addition, as opposed to particle feedstock in LMD, wires cannot achieve mechanical consistency, and lacks the greater control in terms of compositional adjustments in WAAM.

PBF and DED are often compared in terms of parameters such as deposition and energy efficiency [12]. Deposition efficiency in WAAM can reach as much as 100%, which is one of primary reasons for its choice over LMD (14%) for some alloys [13,14]. The overall energy efficiency in WAAM is also found to be greater than LMD (50%), and reach as much as 90% [14]. Figure 1 shows images of the LMD and WAAM machines used in this study to manufacture the samples.

This paper presents an overview of recent advances in 3D printing of composite materials using LMD and WAAM technologies, focusing on mechanical properties and microstructural features of the printed materials. Some of our original work on materials listed in Table 1 using these technologies will also be discussed, while Table 2 specifies the processing conditions.

TABLE 1

List of samples prepared using LMD and WAAM

Sample No.	Sample	Process	Hardness Hv	Remark
1	Ti-6Al-4V	LMD	~345	Good bonding, some inclusions in some samples.
2	SS 316L	LMD	~156	Good reaction and bonding.
3	Al-12Si	LMD	~95	Homogeneous structure with porous content.
4	Al-5356	WAAM	~110	Good bonding
5	CuAl8Ni2	WAAM	~180	Good bonding and grain structure.

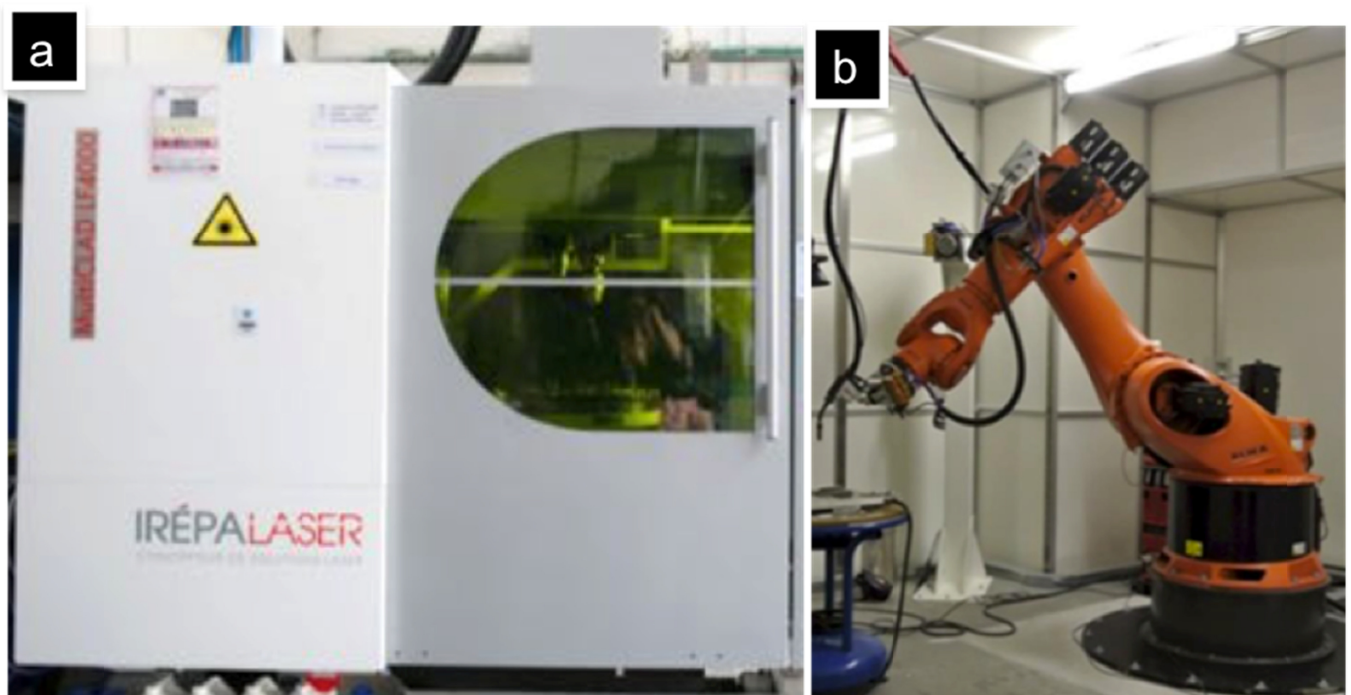


Fig. 1. Images of a) LMD and b) WAAM machines used to prepare Ti, Al and Steel composite [15]

TABLE 2

Processing conditions of WAAM and LMD

Processing conditions of WAAM			Processing conditions of LMD	
Wire material (JIS)	Al-Bronze	Al 5356	Laser power (W)	650-690
Current, A	156	96	Scan speed (mm/min)	2000-2500
Voltage, V	13.4	9.8	Powder flow rate (g/min)	1.6-1.7
Feed speed, m/min	6	7	Vertical increment Δz (mm)	0.16
Travel speed, mm/min	700	700	Number of layers	Variable
Wave pulse, Hz	50-60	50-60	Workspace (mm)	900*900*900
Wire diameter, mm	1.2	1.2		
Shield gas flow rate, l/min	18	18		

2. Advances in Laser Metal Deposition (LMD)

Zhang et al. [6] used a four-component LMDS setup with energy supply, powder delivery, motion and computer control systems in place, to work on commercially available SS 316 with a powder size of 200 mesh, plated onto an A3 steel. As part of the orthogonal experiment with three factors and five levels, the laser power was varied between 600 and 1400 W; scanning speed ranged from 2 to 10 mm/s; and the powder flow rate was altered from 4 to 20 g/min. Nozzle to component surface distance, flow of powder and shielding gas, and translation speed were also varied, keeping in mind that changes in process parameters will directly influence the cladding layers, and the overall quality of the samples in terms of mechanical properties and microstructure. The presence of bright white bands within bonding zone, which lies between the substrate and cladding layers, indicated strong metallurgical bonding within the structure. Furthermore, the typical slender dendritic morphology in the microstructure is directly related to solidification and cooling rate. With the increase in cooling rate, finer dendritic structures were observed ensuring uniform compositional distribution, and without dendrite-dendrite compositional segregation. This fine dendritic microstructure indicates enhanced mechanical behaviours such as strength and hardness. With the increase in scanning speed, most mechanical properties observed an incremental pattern, with Vickers Hardness reaching 360 VHN, yield and tensile strength demonstrating 600 and 690 MPa respectively, and elongation reaching a maximum of 24%.

Reichardt et al. [16] also used a similar system to conduct an interesting study where functionally graded Ti-6Al-4V was deposited on a 304 SS plate with incremental vanadium based interlayers. The process parameters were kept constant in this study. Ti-6Al-4V with a mesh size of 80-325 and particle size of 44-177 μm was first transitioned to Vanadium with mesh size of 60-325, and finally to 304 steel with a mesh size of 140-325.

Several layers were created with increasing vanadium content to the point where the Ti alloy was completely replaced by 304 steel. The experiment was carried out using a minimum laser power of 600 W. The inclusion of Vanadium powders caused powder segregation and exhibited vanadium-rich areas. These areas were also found to contribute towards formation of brittle sigma phases along the height of the samples, deteriorating the mechanical properties of the alloy. To reduce the adverse affect of vanadium inclusion, a greater laser power was recommended to ensure better powder mixing and adequate melt pool temperatures. Within adjacent layers, the presence of small amounts of Fe and Ti was found to be responsible for formation of the brittle intermetallic FeTi phase, creating mid-fabrication cracking. It was found to be difficult to create smooth gradients between SS and V layers due to the presence of the Fe-V-Cr brittle sigma phase.

Dinda et al. [17] fabricated a series of defect-free INCONEL 625 superalloys using laser metal deposition process. The samples observed did not demonstrate cracking between layers, or along the gradient, and displayed extremely low porosity content. The columnar dendritic structures that were seen as part of the microstructure grew vertically from the substrate. The structures demonstrated stability even at temperatures as high as 1000 °C, although increasing the temperature beyond that point resulted in the presence of recrystallized equiaxed phases. The fine microstructure also ensured high and consistent hardness and fracture toughness in the samples, which is highly desired in LMD-ed materials.

Using LMD, the authors have successfully fabricated a range of composite materials [18-20] including Ti-6Al-4V, SS 316L and Al-12Si. A manufacturing route that requires a continuous distribution of materials in powder form, has a direct correlation to the strategy of using and optimising the process parameters, which have been previously detailed [19]. Fig. 2 (a-c) shows images of Ti-6Al-4V, SS 316L and Al-12Si samples. Fig. 2(d) shows a scanning electron micrograph focusing on a pure Ti-6Al-4V region. The flaky columnar pattern is typically seen in LMD alpha-beta titanium alloys [21-24]. It can be seen that large columnar prior beta grains are growing along the z direction (ie in the direction of building across multiple deposited layers). Since the process requires rapid solidification of the material, the cooling cycle goes through what's called a beta transus temperature, where nucleation takes place followed by massive grain growth [16]. While prior beta grains are analysed, a fine acicular structure, which is also known as the Widmanstätten structure, is observed. Presence of such structure in Ti alloys is indicative of high cooling rates [6]. Fig. 2(e) shows an optical micrograph of an LMD-manufactured Al-12Si sample. It shows the presence of porosity across the surface of the sample even though it displayed consistency in terms of homogeneity of pores and pore shape. It also demonstrates the consistent dendritic structures throughout the surface of the sample. The fact that the porosity content was not able to affect the growth and columnar structure of the dendrites ensures high structural integrity, resulting in expected high mechanical strength.

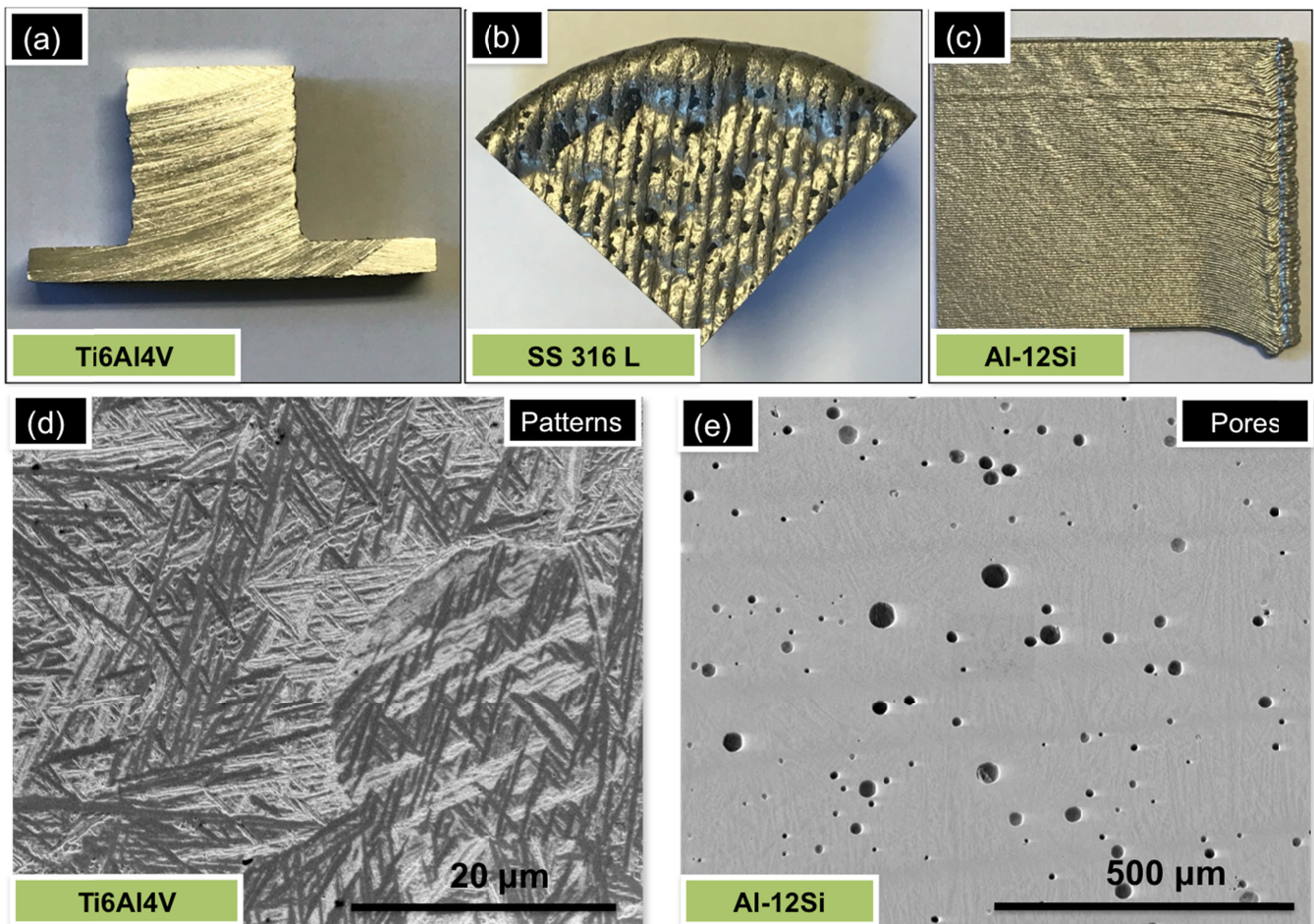


Fig. 2. Images of laser metal deposited a) Ti-6Al-4V b) SS 316 L and c) Al-12Si samples. A scanning electron micrograph in secondary electron beam shows a columnar structure in (d). A homogeneously distributed porous structure is observed in an LMD-ed Al-Si sample (e).

3. Advances in Wire and Arc Additive Manufacturing (WAAM)

Abe et al. [12] conducted a research study where a four axis wire and arc AM machine was used to join two dissimilar materials. First a weld bead of stainless steel YS308L was layered on a substrate composed of SUS304 stainless steel. Finally a Nickel-based alloy Ni6082 was layered on top of YS308L. The microstructure and mechanical properties of both layers and their welded interface were also observed. While a combination of austenite and ferrite were observed on the steel welded layer, dendritic structures were mostly found in Ni6082, which is typical in both of these alloys if normally welded. The interface of these two alloys was well-bonded with presence of no welding defects along the joining line. Due to localised heating, some large grains were found in the steel microstructure. The bonding strength between these two materials is comparable to the tensile strengths of these materials if welded. One of the important findings of this research was to understand the idea that through this nature of joining dissimilar materials, the structure would be highly resistant to heat and corrosion, while ensuring low weight due to the internal rib structure of the 3D printed materials.

In another study, Shen et al. [25] used a WAAM system with two feed wires of 1080 Al and LS422750/4 99.5% Fe in annealed condition. The feed was controlled in a way to maintain 25% Al content in the composition, aiming for a Fe_3Al based intermetallic, which is well known from the Fe-Al binary phase diagram. The study found that it is feasible to fabricate iron-based intermetallics that would demonstrate compositional consistency and homogeneity throughout the structure. Using in situ alloying of Fe and Al in elemental form, it was possible to achieve full density in all layers of the structure, with higher yield strength than what is found in conventionally welded Fe_3Al -based iron aluminide.

One of the major microstructural flaws in conventional welding is the resultant solidified defect or porosity content due to the high thermal input, and affects the mechanical behaviour of the material. To address this limitation WAAM methods have been used to produce large Aluminium parts in an attempt to significantly reduce the porosity content. To reduce the porosity content to the point of eliminating it completely, a further modification on WAAM-manufactured Al has been suggested in the study conducted by Gu et al. [26], where a cold metal transfer process is suggested on Al or its alloys. Using the low heat input of this modified gas arc welding technique, the authors were able to fabricate fully dense Al components, with the presence of

fine equiaxed grains and uniformly distributed θ -Al₂Cu phases in WAAM deposits. The plastic deformation behaviour of the samples studied was also found to be excellent.

Both WAAM and LMD have been extensively used in the fabrication of both large and small components comprised of Ti-6Al-4V. One of the major challenges in working with this alloy has been to controlling the epitaxial growth of coarse primary columnar β -Ti grains in Ti-6Al-4V, that form due to the high heat exposure the material experiences followed by rapid solidification. In addition, the presence of twinning behavior in the microstructure also contributes towards the overall strength reduction of the material. To address these issues, Bermingham et al. [27] conducted a study where traces of Boron were added as part of the molten material, which would later work as a grain growth inhibitor. The additions were found to have great effect on the β -Ti grain morphology as it helped create a barrier around the Ti grains between β -Ti, and Al and V solutes, which would otherwise promote lateral columnar nucleation and growth.

Fig. 3(a, b) shows two samples, Al-5356 and Al Bronze, both fabricated using WAAM. An SEM image of the Al Bronze sample in Fig. 3(c) shows that the grains were properly bonded within the structure. Although there are irregularities in terms of grain size, the porosity content in Al Bronze is quite low, which indicates an excellent bond strength has been achieved during manufacture. The irregularity in grain size can be attributed to the zonal reheating followed by rapid solidification in the layers as no grain growth inhibitors were used; a behavior that is confirmed in several research studies [28-31]. Figure 3 (d) shows a porous segment of Al-5356 microstructure. While porosity can reduce the overall strength of the material, they do not seem to have affected the grains around them to bond between the layers. Grain size refinement is an area of work that needs much attention to address the presence of porous structures in additive manufacturing.

Overall, the mechanical properties in composite materials are heavily influenced by factors such as compositional differences, microstructural features, morphology, crystal structure

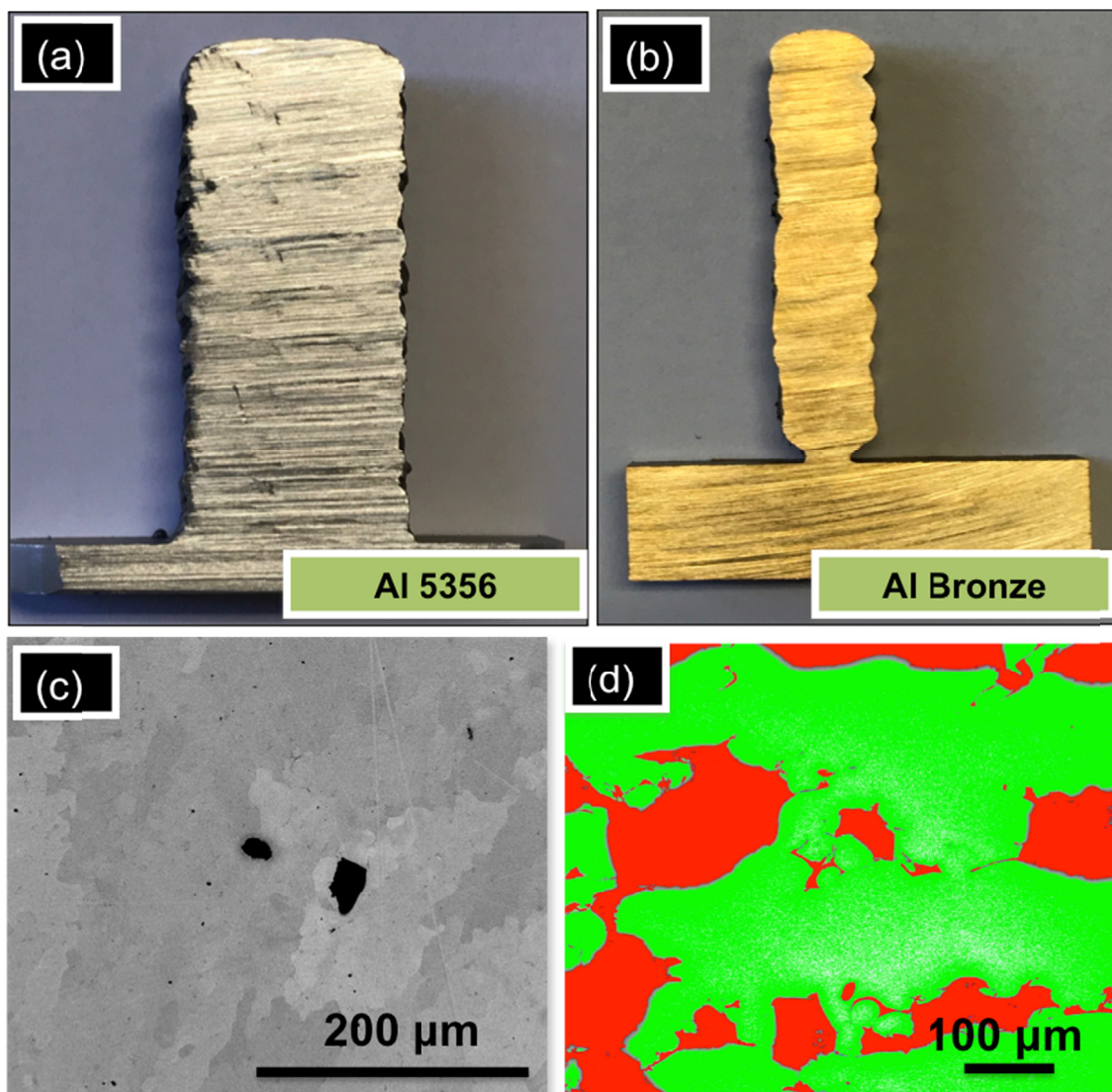


Fig. 3. Images of WAAM samples a) Al-5356 b) Al Bronze (c) A scanning electron micrograph in secondary electron beam shows well bonded grains in Al-Bronze sample. (d). Porosity content in some section WAAM-ed Al alloys, quantitatively measured using Carl Zeiss image processor

and texture, grain size, homogeneity of discontinuities, residual stress and spatial gradients [32]. In additive manufacturing, most of these characteristics are related to the transport and metallurgical phenomena of diffusion, melting, solidification, and solid to liquid phase transformations. Since WAAM and LMD involve these complex interacting phenomena, causing differences in behavior between each sample produced, a better understanding of the influence of these parameters is worthwhile to explore further.

4. Conclusions

One of the major challenges in manufacturing the range of alloys discussed in this paper using LMD or WAAM is to ensure that the structural integrity does not get compromised due to factors such as grain growth, excessive porosity content or partial diffusion and segregation then bonding between materials and layers. Some of the most successful studies indicate that grain growth can be controlled through faster diffusion and rapid heating of these additive-manufacturing processes, while others recommend variation of the control parameters during manufacture. Between the two additive manufacturing technologies, WAAM clearly succeeds in terms of deposition efficiency, whereas LMD takes advantage of its capability to ensure better adhesion between layers. It was also found that the presence of homogeneously distributed columnar and dendritic structures throughout the surface of the samples can offer mechanical consistency and high strength in both LMD and WAAM-ed products. Each technique in additive manufacturing method is potentially the better choice, depending upon the requirements of the 3D printed material in its particular application.

REFERENCES

- [1] H. Lipson, M. Kurman, *Fabricated: The new world of 3D printing*, John Wiley & Sons, 2013.
- [2] W.E. Frazier, *Journal of Materials Engineering and Performance* **23**, 1917-1928 (2014).
- [3] M. Marya, V. Singh, S. Marya, J.Y. Hascoet, *Metallurgical and Materials Transactions B* **46**, 1654-1665 (2015).
- [4] M. Marya, V. Singh, Y. Lu, J.-Y. Hascoet, S. Marya, in: *TMS 2015 144th Annual Meeting & Exhibition*, Springer pp. 413-420, 2015.
- [5] H. El Cheikh, B. Courant, J.-Y. Hascoët, R. Guillén, *Journal of materials processing technology* **212**, 1832-1839 (2012).
- [6] K. Zhang, S. Wang, W. Liu, X. Shang, *Materials & Design* **55**, 104-119 (2014).
- [7] S.W. Williams, F. Martina, A.C. Addison, J. Ding, G. Pardal, P. Colegrove, *Materials Science and Technology* **32**, 641-647 (2016).
- [8] J. Gordon, C. Haden, H. Nied, R. Vinci, D. Harlow, *Materials Science and Engineering: A*, **724**, 431-438 (2018).
- [9] J.-Y. Hascoët, J. Parrot, P. Mognol, E. Willmann, *Welding in the World* **62**, 249-257 (2018).
- [10] A. Queguineur, G. Rückert, F. Cortial, J. Hascoët, *Welding in the World* **62**, 259-266 (2018).
- [11] B. Yin, H. Ma, J. Wang, K. Fang, H. Zhao, Y. Liu, *Materials Letters* **190**, 64-66 (2017).
- [12] T. Abe, H. Sasahara, *Precision Engineering* **45**, 387-395 (2016).
- [13] R. Unocic, J. DuPont, *Metallurgical and materials transactions B* **35**, 143-152 (2004).
- [14] D. Ding, Z. Pan, D. Cuiuri, H. Li, *The International Journal of Advanced Manufacturing Technology* **81**, 465-481 (2015).
- [15] R. Ponche, O. Kerbrat, P. Mognol, J.-Y. Hascoet, *Robotics and Computer-Integrated Manufacturing* **30**, 389-398 (2014).
- [16] A. Reichardt, R.P. Dillon, J.P. Borgonia, A.A. Shapiro, B.W. McEnerney, T. Momose, P. Hosemann, *Materials & Design* **104**, 404-413 (2016).
- [17] G. Dinda, A. Dasgupta, J. Mazumder, *Materials Science and Engineering A* **509**, 98-104 (2009).
- [18] J.-Y. Hascoet, S. Marya, M. Marya, V. Singh, *Proceedings of the 1st International Conference on Progress in Additive Manufacturing* **5**, 133-137 (2014).
- [19] P. Muller, P. Mognol, J.-Y. Hascoet, *Journal of Materials Processing Technology* **213**, 685-692 (2013).
- [20] H. El Cheikh, B. Courant, S. Branchu, X. Huang, J.-Y. Hascoët, R. Guillén, *Optics and Lasers in Engineering* **50**, 1779-1784 (2012).
- [21] L. Ladani, J. Razmi, S.F. Choudhury, *Journal of Engineering Materials and Technology* **136**, 031006 (2014).
- [22] R.M. Mahamood, E.T. Akinlabi, M. Shukla, S. Pityana, *Materials & Design* **50**, 656-666 (2013).
- [23] C. Qiu, G. Ravi, C. Dance, A. Ranson, S. Dilworth, M.M. Attallah, *Journal of Alloys and Compounds* **629**, 351-361 (2015).
- [24] L. Bian, S.M. Thompson, N. Shamsaei, *Jom* **67**, 629-638 (2015).
- [25] C. Shen, Z. Pan, Y. Ma, D. Cuiuri, H. Li, *Additive Manufacturing*, 720-26 (2015).
- [26] J. Gu, B. Cong, J. Ding, S.W. Williams, Y. Zhai, in: *Proceedings of the 25th Annual International Solid Freeform Fabrication Symposium*, Austin, TX, USA, 2014, pp. 4-6.
- [27] M. Bermingham, D. Kent, H. Zhan, D. StJohn, M. Dargusch, *Acta Materialia* **91**, 289-303 (2015).
- [28] F. Wang, S. Williams, M. Rush, *The international journal of advanced manufacturing technology* **57**, 597-603 (2011).
- [29] F. Wang, S. Williams, P. Colegrove, A.A. Antonysamy, *Metallurgical and Materials Transactions A* **44**, 968-977 (2013).
- [30] P. Kobryn, E. Moore, S. Semiatin, *Scripta Materialia* **43**, 299-305 (2000).
- [31] E. Brandl, A. Schoberth, C. Leyens, *Materials Science and Engineering A* **532**, 295-307 (2012).
- [32] A. Antonysamy, University of Manchester, (2012).

APPENDIX 1

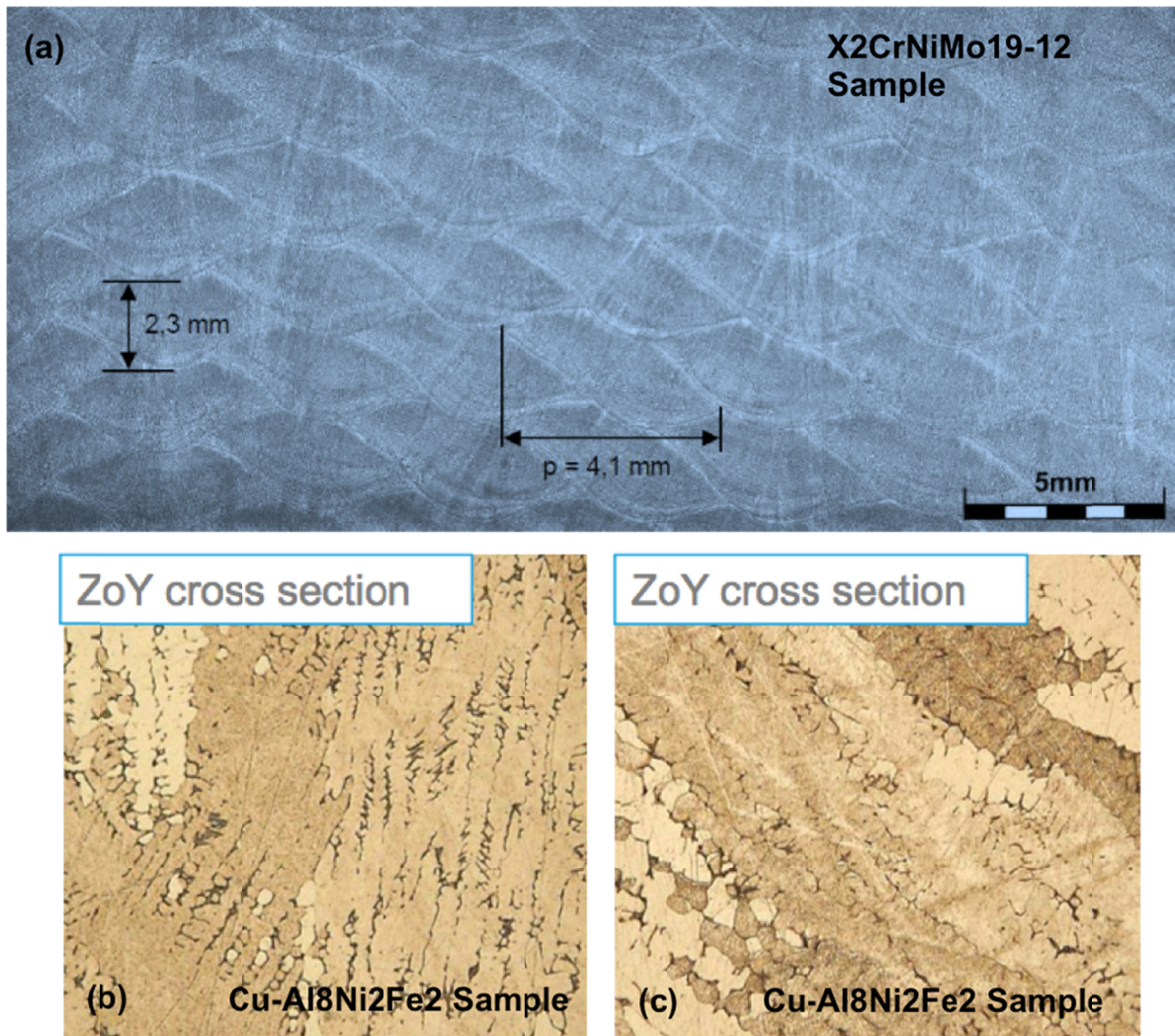


Fig: (a) Micrograph of X2CrNiMo19-12 samples fabricated using WAAM process. It can be seen in the image that the sample displays a consistent presence of the dendritic structure with an average of 8% ferrite FN. No major defects such as lack of fusion, shrinkage, and porosity were observed on the sample. Some micro-oxides (5-10 μm) or cavities (40 μm) were observed in most samples. (b, c) Micrographs of Cu-Al8Ni2Fe2 samples showing consistent presence of dendritic α phase, ensuring high mechanical strength. Some interdendritic $\alpha + \gamma_2$ phase (eutectoid) were also observed in samples. No major defects such as lack of fusion, shrinkage, and porosity were noticed. The samples also demonstrated limited effects of thermal treatment.